

Fine Mapping of “Mini-Muscle,” a Recessive Mutation Causing Reduced Hindlimb Muscle Mass in Mice

JOHN HARTMANN, THEODORE GARLAND JR, ROBERT M. HANNON, SCOTT A. KELLY, GLORIA MUÑOZ, AND DANIEL POMP

From the Department of Nutrition, University of North Carolina, Chapel Hill, NC 27599 (Hartmann, Muñoz, and Pomp); the Department of Biology, University of California, Riverside, CA 92521 (Garland, Hannon, and Kelly); the Department of Cell and Molecular Physiology, Carolina Center for Genome Sciences, University of North Carolina, Chapel Hill, NC 27599 (Pomp).

Address correspondence to D. Pomp at the address above, or e-mail: dpomp@unc.edu.

Prolonged selective breeding of Hsd:ICR mice for high levels of voluntary wheel running has favored an unusual phenotype (mini-muscle [MM]), apparently caused by a single Mendelian recessive allele, in which hindlimb muscle mass is reduced by almost 50%. We recently described the creation and phenotypic characterization of a population suitable for mapping the genomic location of the MM gene. Specifically, we crossed females from a high-runner line fixed for the MM allele with male C57BL/6j. F1 males were then backcrossed to the MM parent females. Backcross (BC) mice exhibited a 50:50 ratio of normal to MM phenotypes. Here, we report on linkage mapping of MM in this BC population to a 2.6335-Mb interval on MMU11. This region harbors ~100 expressed or predicted genes, many of which have known roles in muscle development and/or function. Identification of the genetic variation that underlies MM could potentially be very important in understanding both normal muscle function and dysregulation of muscle physiology leading to disease.

Prolonged selective breeding of Hsd:ICR mice for high levels of voluntary wheel running has favored an unusual phenotype (mini-muscle [MM]), apparently caused by a single Mendelian recessive allele, in which hindlimb muscle mass is reduced by almost 50%. This phenotype was originally observed in 2 of 4 replicate selected lines (termed HR for high runner) and in 1 of 4 control (nonselected) lines (Garland et al. 2002). Analyses of data from the first 22 generations of the selection experiment indicated that the mutant allele was present at a frequency of approximately 7% in the base population (outbred Hsd:ICR mice). Five of the 8 total lines apparently lost the allele by random genetic drift. In one control line, the phenotype, representing homozygotes, was observed at a frequency of 0–10% for the

first 22 generations (Garland et al. 2002) and was then apparently lost (T Garland Jr. unpublished observations). The 2 selected lines that have exhibited the phenotype showed an increase in frequency consistent with positive selection (Garland et al. 2002). In one (lab designated line 6), the phenotype remains polymorphic as of generation 50. In the other (lab designated line 3), the mutation apparently had gone to fixation by generation 36 (Syme et al. 2005).

The most characteristic phenotype of MM allele homozygotes is a 50% reduction in mass of the triceps surae muscle complex (Garland et al. 2002) as well as in mass of mixed hindlimb muscle exclusive of the triceps surae (Houle-Leroy et al. 2003). Beyond this, the MM allele has many pleiotropic effects in homozygotes, including a doubling of mass-specific aerobic capacity as compared with wild-type muscle (Houle-Leroy et al. 2003), altered fiber type composition in the gastrocnemius (Guderley et al. 2008), altered muscle contractile performance (Syme et al. 2005), an increase in size of their ventricles, liver, and spleen (Garland et al. 2002; Swallow et al. 2005), and longer and thinner hindlimb bones (Kelly et al. 2006). Many of these effects seem conducive to the support of endurance running (Garland 2003; Guderley et al. 2006; Rezende et al. 2006). To date, clearly deleterious consequences of the MM allele have not been reported.

Although the physiological consequences of MM are becoming well understood, the nature of the underlying mutation has not been characterized. Identification of the MM gene, and how variation within that gene leads to the MM phenotype, would be important for understanding both normal and abnormal muscle development in mammalian species. We recently described the creation and phenotypic characterization of a population suitable for mapping the genomic location of the MM gene (Hannon et al. 2008). We crossed females from the HR line that is fixed for the MM

allele with male C57BL/6J. F1 males were then backcrossed to the MM parent females. The HR(B6HRF1) backcross (BC) mice ($N = 404$) were dissected, and a 50:50 ratio of normal to MM phenotype was observed. In this paper, we report on linkage mapping of MM in this BC population to a 2.6335-Mb interval on MMU11. This region harbors ~100 expressed or predicted genes, many of which have known roles in muscle development and/or function.

Methods

Development of BC Mapping Population

As described elsewhere (Hannon et al. 2008), 20 C57BL/6J males (The Jackson Laboratory, Bar Harbor, ME) were harem mated with each of 3 females from HR line 3, which is apparently fixed for the MM mutant allele (Syme et al. 2005). Sixty male F1 mice were weaned at 21 days of age. At approximately 8 weeks of age, they were randomly backcrossed (one dam with one sire) to the HR line 3 dams, with the exception that mother–son and aunt–nephew matings were disallowed. Once dams were visually pregnant, F1 males were removed. The HR(B6HRF1) BC pups were weaned at 21 days, then all line 3 dams and F1 males were dissected following Garland et al. (2002) to determine MM phenotype status (see below).

When BC pups reached approximately 7 weeks of age, they were given 6 days of wheel access (as in the routine selective breeding protocol described by Swallow et al., 1998) and then dissected to determine MM phenotype. For mice in all 4 groups (C57BL/6J males, HR line 3 females, F1 offspring, and BC offspring), plots of mean triceps surae muscle mass against body mass allowed unambiguous identification of MM individuals (Figure 1).

Chromosomal Localization and Fine Mapping of MM

General Methods

Microsatellite marker analysis was performed in 2 overall steps. An initial genome-wide scan was performed with sparse genome coverage using 54 BC mice segregating for MM, to identify the general chromosomal region harboring the MM gene. This was followed by fine mapping with dense marker coverage within the MM region using all BC mice. Microsatellite markers were genotyped as previously described (Allan et al. 2005). Linkage maps were constructed using MAP MANAGER QTX (<http://www.mapmanager.org/mmQTX.html>). For all linkage estimations, genotypes for MM were inferred based on phenotypic evidence as described above. BC mice with MM were designated mini/mini, whereas mice with no evidence of MM were designated mini/B6.

Sparse Mapping

Because HR has not been previously genotyped for microsatellite markers, and is not fully inbred, we initially tested several markers on each autosome for informativeness in the BC. Two or 3 microsatellite markers (total of 48)

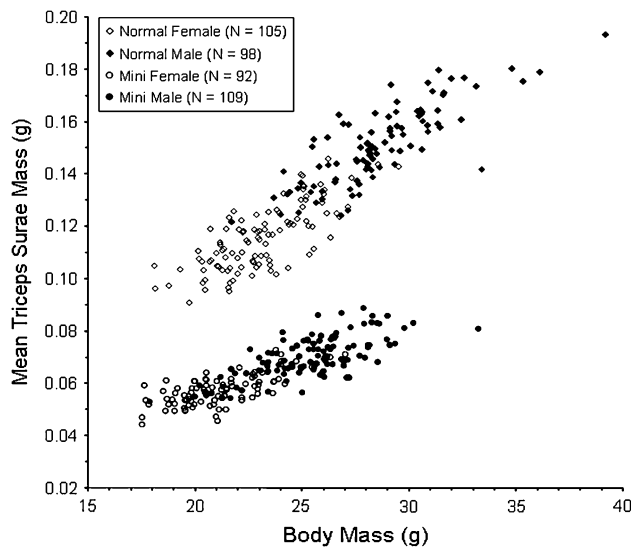


Figure 1. Relation between triceps surae mass (mean of left and right) and body mass for HR(B6HRF1) BC mice. The MM phenotype, characterized by a nearly 50% reduction in muscle mass, was found in ~50% of BC mice, supporting a single recessive locus model.

across all 19 autosomes were selected for the scan (data not shown). These were genotyped across a subset of 54 BC mice having a 50:50 ratio of MM and normal phenotypes selected across several BC families. A Chi-square test was used to test for significant ($P < 0.05$) linkage between a microsatellite marker and the mutant gene, by examining deviations from the expectation that 50% of the samples should have a mini/mini marker genotype and 50% should have a mini/B6 genotype.

Fine Mapping

Initially, markers *D11Mit108*, *D11Mit260*, *D11Mit141*, and *D11Mit212*, all found to be informative in the initial marker testing, were genotyped across the full BC population of 404 mice, and a linkage map was generated for these 4 markers and MM. For further fine mapping, additional markers were tested in the region between 37.0 and 43.8 cM (Table 1). From this test, an additional 3 markers (*D11Mit4*, *D11Mit31*, and *D11Mit90*) were selected and genotyped in the full BC and a new linkage map was generated based on 7 microsatellite markers and MM.

Subsequently, additional informative markers were genotyped but only in specific BC mice harboring a recombination near the estimated linkage position of MM. New markers were genotyped in the regions between *D11Mit260* (34.4 cM, 61.61 Mb) and *D11Mit4* (37.0 cM, 68.42 Mb) and between *D11Mit31* (40.0 cM) and *D11Mit90* (42.0 cM, 70.31 Mb). When no previously published markers were available, primers were designed flanking putative microsatellites identified through BLAST searches in Ensembl and informative markers were genotyped. This process was continued until nearly all information on

Table 1. All markers used in microsatellite mapping of MM

Marker	Chromosome	Linkage position (cM)	Physical position (Mb)	Phase of mapping
<i>D1mit318</i>	1	18.5	33.84	Sparse mapping
<i>D1mit33</i>	1	81.6	160.34	Sparse mapping
<i>D1mit128</i>	1	36.9	72.57	Sparse mapping
<i>D2mit297</i>	2	29.0	42.46	Sparse mapping
<i>D2mit171</i>	2	98.0	34.34	Sparse mapping
<i>D3mit203</i>	3	11.2	26.84	Sparse mapping
<i>D3mit147</i>	3	79.4	148.41	Sparse mapping
<i>D4mit171</i>	4	6.3	22.41	Sparse mapping
<i>D4mit139</i>	4	28.6	55.26	Sparse mapping
<i>D4mit71</i>	4	61.9	133.34	Sparse mapping
<i>D5mit126</i>	5	20.0	35.80	Sparse mapping
<i>D5mit240</i>	5	59.0	109.52	Sparse mapping
<i>D6mit119</i>	6	25.5	50.81	Sparse mapping
<i>D6mit31</i>	6	38.5	92.67	Sparse mapping
<i>D6mit217</i>	6	60.5	125.27	Sparse mapping
<i>D7mit227</i>	7	16.0	37.37	Sparse mapping
<i>D7mit321</i>	7	48.5	105.05	Sparse mapping
<i>D8mit64</i>	8	16.0	33.90	Sparse mapping
<i>D8mit215</i>	8	59.0	118.38	Sparse mapping
<i>D9mit205</i>	9	18.0	37.11	Sparse mapping
<i>D9mit165</i>	9	38.0	68.53	Sparse mapping
<i>D9mit212</i>	9	61.0	108.54	Sparse mapping
<i>D10mit126</i>	10	21.0	26.73	Sparse mapping
<i>D10mit70</i>	10	59.0	103.54	Sparse mapping
<i>D11mit108</i>	11	18.0	35.86	Sparse mapping and initial fine mapping
<i>D11mit141</i>	11	27.0	52.96	Initial fine mapping
<i>D11mit260</i>	11	34.4	61.61	Initial fine mapping
<i>D11Mit115</i>	11	37.0	67.45	Tertiary fine mapping
<i>3D</i>	11	—	67.97	Tertiary fine mapping
<i>D11Mit1000^a</i>	11	—	68.32	Secondary fine mapping
<i>D11Mit4</i>	11	37.0	68.42	Secondary fine mapping
<i>D11mit60</i>	11	40.0	69.55	Tertiary fine mapping
<i>D11mit30</i>	11	39.8	69.61	Tertiary fine mapping
<i>D11mit29</i>	11	40.0	69.61	Tertiary fine mapping
<i>D11mit31</i>	11	40.0	—	Tertiary fine mapping
<i>1F</i>	11	—	70.09	Tertiary fine mapping
<i>1H</i>	11	—	70.09	Tertiary fine mapping
<i>1A</i>	11	—	70.10	Tertiary fine mapping
<i>1B</i>	11	—	70.10	Tertiary fine mapping
<i>D11Mit90</i>	11	42.0	70.31	Secondary fine mapping
<i>D11mit212</i>	11	50.0	88.67	Sparse mapping and initial fine mapping
<i>D12mit185</i>	12	11.0	27.75	Sparse mapping
<i>D12mit153</i>	12	15.0	35.92	Sparse mapping
<i>D12mit156</i>	12	34.0	80.56	Sparse mapping
<i>D12mit158</i>	12	38.0	83.72	Sparse mapping
<i>D13mit158</i>	13	5.0	49.33	Sparse mapping
<i>D13mit198</i>	13	7.7	35.06	Sparse mapping
<i>D13mit139</i>	13	32.0	51.86	Sparse mapping
<i>D13mit202</i>	13	47.0	91.61	Sparse mapping
<i>D14mit141</i>	14	15.0	47.38	Sparse mapping
<i>D14mit82</i>	14	19.5	53.41	Sparse mapping
<i>D14mit196</i>	14	47.0	—	Sparse mapping
<i>D15mit12</i>	15	4.7	31.61	Sparse mapping
<i>D15mit107</i>	15	49.0	84.22	Sparse mapping
<i>D16mit132</i>	16	3.7	—	Sparse mapping
<i>D16mit71</i>	16	70.7	97.13	Sparse mapping
<i>D17mit175</i>	17	17.7	—	Sparse mapping
<i>D17mit72</i>	17	47.4	79.39	Sparse mapping
<i>D18mit123</i>	18	31.0	56.13	Sparse mapping
<i>D18mit4</i>	18	57.0	84.30	Sparse mapping
<i>D19mit128</i>	19	10.9	17.33	Sparse mapping
<i>D19mit67</i>	19	43.0	44.47	Sparse mapping
<i>D19mit71</i>	19	54.0	59.67	Sparse mapping

^a *D11Mit1000* is named *D17Mit144* in the Ensembl database.

Table 2. Chi-square values for 2 markers on Chromosome 11 in the genome-wide screen of 54 BC mice

Marker	Position (cM)	Physical location (Mb)	MM mice		Normal mice		Chi square
			Mini/mini	Mini/B6	Mini/mini	Mini/B6	
<i>D11Mit108</i>	18	35.86	24	6	4	20	9.48
<i>D11Mit212</i>	50	88.67	23	6	4	21	10.7

location of recombinations in the BC was exhausted. A total of 17 newly designed markers were tested, of which 15 amplified well and 5 were informative (Table 1).

Candidate Gene Sequencing

DNA from C57BL/6J ($n = 1$), HR Line 3 mice with MM ($n = 3$), HR Line 6 mice with MM ($n = 3$), and HR Line 6 mice without MM ($n = 3$) was used to generate polymerase chain reaction (PCR) products for sequencing of candidate genes within the fine-mapped MM interval. For *sax15*, overlapping PCR products were amplified encompassing the entire gene plus some flanking sequence (Ensembl coordinates: 69,468,319–69,470,660). For *Cbrnb1*, 11 overlapping PCR products were amplified to encompass 4959 bp of the gene including all 11 exons and part of the 5' and 3' untranslated region (UTR) regulatory sequences (Ensembl coordinates 69,609,023–69,609,447; 69,608,428–69,608,582; 69,607,330–69,607,783; 69,606,871–69,607,171; 69,606,147–69,606,445; 69,600,313–69,600,624; 69,599,120–69,599,461; 69,598,235–69,598,730; 69,597,890–69,598,334; 69,597,558–69,598,061; 69,597,174–69,597,674). For *rpl26*, overlapping PCR products were amplified representing the entire gene (Ensembl coordinates: 68,715,068–68,718,035). All PCR products incorporated 5' and 3' M13 tails and were sequenced from both directions through a service provider (Agencourt Bioscience, Beverly, MA).

Results

Sparse Mapping

Two microsatellite markers on MMU11 (*D11Mit108*, 18 cM, 36 Mb and *D11Mit212*, 50 cM, 89 Mb) were found to be linked with MM ($P < 0.01$; Table 2) based on genotyping of 54 BC mice. Given that the estimated strength of linkage between MM and each of these markers was very similar (Table 2), the position of MM was presumed to be near the midpoint of the markers at ~ 35 cM. No markers on other chromosomes showed significant linkage to MM.

Fine Mapping

Results of initial linkage mapping using MM and 4 microsatellite markers genotyped across the full BC population are summarized in Table 3. The estimated positions are given as ranges. MM mapped between markers *D11Mit260* (34.4 cM, 61.6 Mb) and *D11Mit212* (50 cM, 88.7 Mb). Location of MM was estimated to be 4.45 cM distal to *D11Mit260* and 9.83 cM proximal to *D11Mit212*.

After genotyping of 3 additional markers (*D11Mit4*, *D11Mit31*, and *D11Mit90*), only one (*D11Mit90*, 42 cM, 70.32 Mb) revealed new recombinations for linkage mapping. Results of the new mapping including this additional marker are summarized in Table 4 and Figure 2, showing that the region harboring MM had now been effectively reduced to the interval of 61.6–70.3 Mb. The very tight linkage (0.5 cM) between MM and *D11Mit90* provided evidence that MM was likely near the distal edge of this interval.

For further fine mapping of the MM mutation, only mice with recombinations between MM and *D11Mit260* on the proximal end ($n = 18$) or *D11Mit90* on the distal end ($n = 2$) were genotyped. Given that no new estimations of linkage would be feasible, only physical locations were used at this point to guide selection and/or design of additional microsatellite markers. New genotyping within this region revealed additional recombinations, helping to further refine the localization of MM (Table 5), with new boundaries of *D11Mit115* (67.453 Mb) and the newly designed marker 1F (70.0865). Having exhausted recombinations in this BC population, MM was localized to this 2.6335-Mb region, which harbors ~ 100 genes (Table 6; NCBI Build 37.1 [February, 2008]).

Candidate Gene Sequencing

Three genes within the 2.6335-Mb region harboring MM were selected for sequencing based on having well-characterized roles in muscle development. For *sax15*, no genetic variation was observed across the entire gene sequence between any of the samples. For *cbrnb1*, 2 single nucleotide polymorphisms and a 3-bp deletion (GGA/-) were observed between C57BL/6J and HR mice within the 3' UTR (data not shown). However, none of the sequence variants found within *cbrnb1* correlated with the MM phenotype within HR mice. For *rpl26*, many polymorphisms

Table 3. Initial fine mapping linkage map between MM and 4 microsatellite markers

Marker	Linkage distance (cM)	MGD position (cM)	Physical location (Mb)
<i>D11Mit108</i>		18.0	35.86
	5.49		
<i>D11Mit141</i>		27.0	52.96
	6.21		
<i>D11Mit260</i>		34.4	61.61
	4.45		
<i>Mini-Muscle</i>		—	—
	9.83		
<i>D11Mit212</i>		50.0	88.67

MGD, mouse genome database.

Table 4. Linkage map after secondary phase of fine mapping

Marker	Linkage distance (cM)	MGD position (cM)	Physical location (Mb)
<i>D11Mit108</i>		18.0	35.86
	5.49		
<i>D11Mit141</i>	6.21	27.0	52.96
<i>D11Mit260</i>		34.4	61.61
	4.53		
<i>Mini-Muscle</i>	0.51	—	—
<i>D11Mit90</i>	9.39	42.0	70.31
<i>D11Mit212</i>		50.0	88.67

MGD, mouse genome database.

were found between C57BL/6J and HR mice (data not shown), but again, none of this genetic variation segregated in a manner that provided evidence for being causal for MM.

Discussion

Mapping and subsequent identification of spontaneous mutations with major phenotypic effect in mice have played

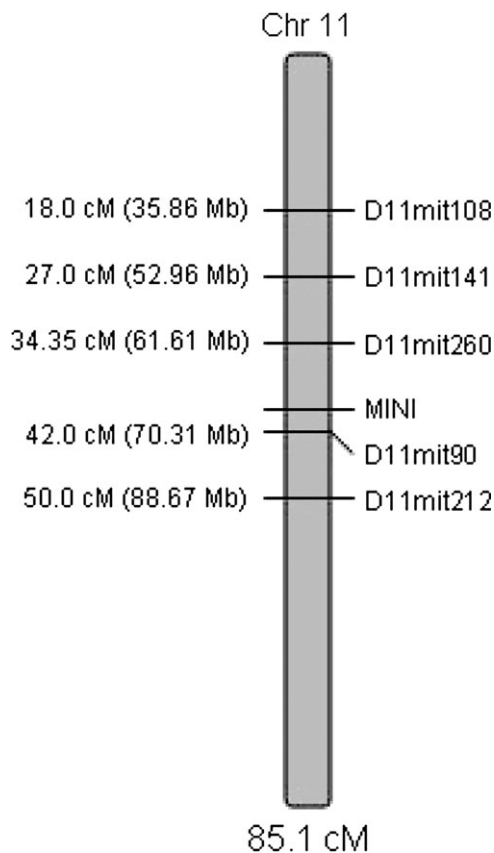


Figure 2. Initial linkage map of the MM region after genotyping of 6 markers on MMU11 in the full HR(B6HRF1) BC population.

Table 5. Genotypic matrix for further fine mapping of MM using 20 informative BC mice

Mouse ID	<i>D11Mit260</i>	<i>D11Mit115</i>	MM	<i>IF</i>	<i>D11Mit90</i>
	61.609 Mb	67.453 Mb	—	70.0865 Mb	70.313 Mb
4302	H	R	R	—	R
4482	H	R	R	—	R
4471	H	R	R	—	R
4472	H	R	R	—	R
4081	H	R	R	—	R
4239	—	R	R	—	R
4196	H	R	R	—	R
4238	R	H	H	—	H
4427	R	H	H	—	H
4276	R	H	H	—	H
4269	R	H	H	—	H
4292	R	H	H	—	H
4279	R	H	H	—	H
4152	R	H	H	—	H
4404	R	H	H	—	H
4268	R	H	H	—	H
4197	R	R	H	—	H
4086	H	H	R	—	R
4199	R	—	R	H	H
4344	H	—	H	H	R

H, mini/B6 genotype; R, mini/mini genotype. Relevant recombinations are in bold.

a significant role in furthering our understanding of many physiological processes. These include growth (e.g., growth hormone–releasing hormone receptor; Godfrey et al. 1993), obesity (e.g., leptin; Zhang et al. 1994), and reproduction (e.g., gonadotropin-releasing hormone; Mason et al. 1986). Spontaneous mutations in genes regulating muscle development have also been identified. For example, the “compact” mutation causing hypermuscularity in mice (Varga et al. 1997) was subsequently identified as a deletion in myostatin (*mstn*) (Szabó et al. 1998), a finding that was driven by the discovery that muscles of myostatin knockout mice weigh 2–3 times more than those of wild-type animals (McPherron et al. 1997). A second example is the “high-growth” mutation, which was first observed because it caused a 30–50% increase in postweaning growth rate of mice (Bradford and Famula 1984). The underlying mutation was later identified as a ~500-kb deletion of a region containing the gene cytokine signaling 2 (*Socs2*), a member of a family of regulators of cytokine signal transduction (Horvat and Medrano 2001).

In this study, we have mapped the recessive MM mutation, which causes most hindlimb muscles to have markedly reduced mass, to a 2.6335-Mb interval on MMU11. Effects of this MM mutation were originally observed in 2 of 4 replicate lines during the course of long-term selective breeding for high levels of voluntary wheel running and in 1 of 4 control (nonselected) lines (Garland et al. 2002). Analyses of data from the first 22 generations of the selection experiment indicated that the mutant allele was present at a frequency of approximately 7% in the base

Table 6. Expressed and predicted genes within the 2.6335 Mb MMU11 region harboring MM

Symbol	Start base pair	Stop base pair	Description
<i>Gas7</i>	67,416,607	67,498,461	Growth arrest specific 7
<i>Rcvm</i>	67,500,799	67,516,835	Recoverin
<i>Glp2r</i>	67,519,932	67,584,655	Glucagons-like peptide 2 receptor
<i>LOC544792</i>	67,588,110	67,603,400	Similar to germ cell associated 1 (predicted)
<i>Dhrs7c</i>	67,611,790	67,629,507	Dehydrogenase/reductase (family) member 7C
<i>LOC100041899</i>	67,651,191	67,657,281	Hypothetical protein LOC100041899
<i>Usp43</i>	67,668,025	67,735,655	Ubiquitin-specific peptidase 43
<i>Wdr16</i>	67,738,308	67,779,144	WD repeat domain 16
<i>Six8</i>	67,779,985	68,020,650	Syntaxin 8
<i>Ntn1</i>	68,022,866	68,200,328	Netrin 1
<i>Pik3r5</i>	68,245,627	68,311,348	Phosphoinositide-3-kinase, regulatory subunit 5, p101
<i>BB220380</i>	68,316,521	68,366,200	Expressed sequence BB220380
<i>BC024997</i>	68,369,688	68,371,747	cDNA sequence BC024997
<i>Ccdc42</i>	68,407,557	68,411,456	Coiled-coil domain containing 42
<i>Myb10</i>	68,505,417	68,630,126	Myosin, heavy polypeptide 10, nonmuscle
<i>Ndel1</i>	68,634,936	68,666,564	Nuclear distribution gene E-like homolog 1 (<i>A. nidulans</i>)
<i>9930039.A11Rik</i>	68,702,055	68,708,517	RIKEN cDNA 9930039A11 gene
<i>Rpl26</i>	68,715,068	68,718,036	Ribosomal protein L26
<i>Odf4</i>	68,735,337	68,740,551	Outer dense fiber of sperm tails 4
<i>Arhgef15</i>	68,756,656	68,770,360	Rho guanine nucleotide exchange factor 15
<i>Slc25a35</i>	68,781,633	68,786,017	Solute carrier family 25, member 35
<i>2400006H24Rik</i>	68,785,989	68,787,322	RIKEN cDNA 2400006H24 gene
<i>Pfas</i>	68,798,671	68,821,962	Phosphoribosylformylglycinamide synthase (amidotransferase)
<i>1500010J02Rik</i>	68,829,615	68,849,972	RIKEN cDNA 1500010J02 gene
<i>Aurkb</i>	68,859,145	68,865,164	Aurora kinase B
<i>2310047M10Rik</i>	68,873,277	68,875,078	RIKEN cDNA 2310047M10 gene
<i>Tmem107</i>	68,884,311	68,886,794	Transmembrane protein 107
<i>Vamp2</i>	68,902,030	68,905,883	Vesicle-associated membrane protein 2
<i>Per1</i>	68,912,451	68,923,462	Period homolog 1 (<i>Drosophila</i>)
<i>Hes7</i>	68,933,955	68,936,761	Hairy and enhancer of split 7 (<i>Drosophila</i>)
<i>Aloxe3</i>	68,939,879	68,962,616	Arachidonate lipoxygenase 3
<i>Alox12b</i>	68,970,574	68,983,293	Arachidonate 12-lipoxygenase, 12R type
<i>Alox8</i>	68,997,387	69,011,341	Arachidonate 8-lipoxygenase
<i>Gucy2e</i>	69,036,537	69,050,147	Guanylate cyclase 2e
<i>Centrob</i>	69,112,998	69,137,277	Centrobin, centrosomal BRCA2-interacting protein
<i>Trappc1</i>	69,137,482	69,139,295	Trafficking protein particle complex 1
<i>Kcnab3</i>	69,139,760	69,146,543	Potassium voltage-gated channel, shaker-related subfamily, beta member 3
<i>A030009H04Rik</i>	69,154,319	69,156,143	RIKEN cDNA A030009H04 gene
<i>Chd3</i>	69,156,775	69,182,928	Chromodomain helicase DNA-binding protein 3
<i>Cyb5d1</i>	69,207,114	69,208,848	Cytochrome b5 domain containing 1
<i>Lsm1</i>	69,209,293	69,210,173	LSM domain containing 1
<i>Tmem88</i>	69,210,021	69,211,736	Transmembrane protein 88
<i>Jmjd3</i>	69,212,010	69,227,177	Jumonji domain containing 3
<i>Dnabc2</i>	69,234,311	69,362,610	Dynein, axonemal, heavy chain 2
<i>Efnb3</i>	69,367,627	69,373,680	Ephrin B3
<i>Wdr79</i>	69,375,256	69,392,826	WD repeat domain 79
<i>LOC100043030</i>	69,387,322	69,387,686	Similar to ribosomal protein S27 (metalloprotein 1)
<i>Trp53</i>	69,393,483	69,405,373	Transformation-related protein 53
<i>Atp1b2</i>	69,413,252	69,419,462	ATPase, Na ⁺ /K ⁺ transporting, beta 2 polypeptide
<i>Sbhg</i>	69,428,318	69,431,370	Sex hormone-binding globulin
<i>Sat2</i>	69,435,611	69,437,371	Spermidine/spermine N1-acetyl transferase 2
<i>LOC382532</i>	69,444,405	69,444,814	Similar to ribosomal protein S15a
<i>Fxr2</i>	69,446,473	69,466,799	Fragile X mental retardation, autosomal homolog 2
<i>Sox15</i>	69,468,875	69,470,123	SRY-box-containing gene 15
<i>Mpdu1</i>	69,470,206	69,476,144	Mannose-P-dolichol utilization defect 1
<i>Cd68</i>	69,477,873	69,479,564	CD68 antigen
<i>Eif4a1</i>	69,480,441	69,485,817	Eukaryotic translation initiation factor 4A1
<i>Senp3</i>	69,486,620	69,495,348	SUMO/sentrin-specific peptidase 3
<i>Tnfrsf13</i>	69,496,079	69,499,056	Tumor necrosis factor (ligand) superfamily, member 13
<i>Tnfrsf12-tnfrsf13</i>	69,496,079	69,509,499	Tumor necrosis factor (ligand) superfamily, member 12-member 13
<i>Tnfrsf12</i>	69,499,850	69,509,256	Tumor necrosis factor (ligand) superfamily, member 12

Table 6. Continued

Symbol	Start base pair	Stop base pair	Description
<i>LOC100041994</i>	69,543,497	69,545,211	Hypothetical protein LOC100041994
<i>Polr2a</i>	69,547,912	69,571,725	Polymerase (RNA) II (DNA directed) polypeptide A
<i>Amac1</i>	69,573,386	69,575,346	Acyl-malonyl-condensing enzyme 1
<i>Zbtb4</i>	69,588,908	69,593,175	Zinc finger and BTB domain containing 4
<i>Chrn1</i>	69,597,539	69,609,445	Cholinergic receptor, nicotinic, beta polypeptide 1 (muscle)
<i>Fgf11</i>	69,611,704	69,615,127	Fibroblast growth factor 11
<i>Tmem102</i>	69,617,105	69,619,126	Transmembrane protein 102
<i>4933402P03Rik</i>	69,630,068	69,631,942	RIKEN cDNA 4933402P03 gene
<i>1700095G12Rik</i>	69,634,373	69,635,667	RIKEN cDNA 1700095G12 gene
<i>Nlgn2</i>	69,636,625	69,648,351	Neuroigin 2
<i>1810027O10Rik</i>	69,652,027	69,653,060	RIKEN cDNA 1810027O10 gene
<i>Plscr3</i>	69,660,178	69,665,560	Phospholipid scramblase 3
<i>Tnk1</i>	69,664,601	69,672,219	Tyrosine kinase, nonreceptor, 1
<i>LOC432576</i>	69,690,186	69,691,607	Hypothetical LOC432576
<i>Kctd11</i>	69,691,179	69,694,908	Potassium channel tetramerisation domain containing 11
<i>Centb1</i>	69,695,069	69,709,041	Centaurin, beta 1
<i>2810408A11Rik</i>	69,710,860	69,714,488	RIKEN cDNA 2810408A11 gene
<i>0610025P10Rik</i>	69,715,393	69,727,322	RIKEN cDNA 0610025P10 gene
<i>Gps2</i>	69,727,694	69,730,093	G-protein pathway suppressor 2
<i>Eif5a</i>	69,730,224	69,734,843	Eukaryotic translation initiation factor 5A
<i>Ybx2</i>	69,749,401	69,755,101	Y-box protein 2
<i>Slc2a4</i>	69,755,788	69,761,692	Solute carrier family 2 (facilitated glucose transporter), member 4
<i>LOC668442</i>	69,764,300	69,764,986	Similar to Cofilin-1 (Cofilin, nonmuscle isoform)
<i>Cldn7</i>	69,779,003	69,781,380	Claudin 7
<i>Rai12</i>	69,781,726	69,794,012	Retinoic acid induced 12
<i>Dullard</i>	6,9794,670	69,804,103	Dullard homolog (<i>Xenopus laevis</i>)
<i>Gabarap</i>	69,804,872	69,808,448	Gamma-aminobutyric acid receptor-associated protein
<i>Phf23</i>	69,809,279	69,813,418	PHD finger protein 23
<i>Dvl2</i>	69,814,128	69,823,611	Disheveled 2, dsh homolog (<i>Drosophila</i>)
<i>Acad11</i>	69,823,694	69,828,909	Acyl-Coenzyme A dehydrogenase, very long chain
<i>Dlg4</i>	69,832,366	69,858,270	Discs, large homolog 4 (<i>Drosophila</i>)
<i>Asgr1</i>	69,867,871	69,871,396	Asialoglycoprotein receptor 1
<i>Asgr2</i>	69,906,146	69,919,689	Asialoglycoprotein receptor 2
<i>Mgl2</i>	69,943,859	69,951,044	Macrophage galactose N-acetyl-galactosamine-specific lectin 2
<i>Mgl1</i>	69,980,276	69,984,336	Macrophage galactose N-acetyl-galactosamine-specific lectin 1
<i>Slc16a11</i>	70,027,582	70,029,915	Solute carrier family 16 (monocarboxylic acid transporters), member 11
<i>Slc16a13</i>	70,030,294	70,034,496	Solute carrier family 16 (monocarboxylic acid transporters), member 13
<i>Bcl6b</i>	70,037,630	70,043,223	B-cell CLL/lymphoma 6, member B
<i>0610010K14Rik</i>	70,048,710	70,051,416	RIKEN cDNA 0610010K14 gene
<i>D11Bwg0434e</i>	70,051,628	70,053,348	DNA segment, Chr 11, Brigham and Women's Genetics 0434 expressed
<i>Alox12</i>	70,054,957	70,068,843	Arachidonate 12-lipoxygenase

Data retrieved from NCBI Build 37.1 (February, 2008).

population (outbred Hsd:ICR mice). It is intriguing that both the compact and high-growth mutations were also originally discovered during the course of long-term selection experiments, for increased carcass protein content (Varga et al. 1997) and rapid weight gain (Bradford and Famula 1984), respectively. It is not known if the compact mutation was segregating in the base population prior to selection. For high growth, the mutation arose spontaneously after more than 20 generations of selection. The appearance of major mutations affecting a trait under selection has been documented many other times, as discussed by Varga et al. (1997). The strong selection intensity placed on quantitative traits during artificial selection experiments is well suited to take advantage of preexisting genetic variation in the base population or newly

created genetic variation during the selection experiment, arising due to spontaneous mutations with major phenotypic effect.

Although our mapping efforts have succeeded in localizing MM to a reasonably small genomic interval, the goal of identifying the genetic variation responsible for the MM phenotype remains a formidable challenge. Mouse chromosome 11 is gene rich, with an average of 14 genes per Mb compared with the genome-wide average of 6.5. However, the 2.6335-Mb MM interval on MMU11 is extremely dense with genes, harboring 102 expressed and predicted genes (NCBI Build 37.1; February, 2008). Furthermore, many of the genes within this region represent viable candidates based on known physiological roles in muscle development. For example, SRY-box containing

gene 15 (*sox15*) plays a role determining the early myogenic cell lineages during mouse skeletal muscle development (Lee et al. 2004). Mutations within cholinergic receptor, nicotinic, beta polypeptide 1 (*chrb1*) have been shown to cause congenital myasthenic syndromes in humans (Quiram et al. 1999), as have mutations within the epsilon subunit (*chrme*), which falls just ~500 kb distal to the MM region. Ribosomal protein L26 (*rpl26*) is very strongly upregulated (~35-fold increase) in satellite cells during muscle regeneration (Kardon G, personal communication). Although we found no causal sequence variation within these 3 genes, additional polymorphisms could exist in regions outside of those in our sequencing design.

In addition to these 3 candidate genes, many of the other ~100 genes in the MM region are expressed in muscle, and the *Acadvl*, *Myb10*, *Sle2a4*, and *Trp53* genes all have effects on muscle when genetically modified (Mouse Genome Informatics database; February, 2008). Many of the genes in this region still have unknown function and may be involved in muscle development or regulation. Further, there are several microRNA genes (*miR-324-3P*, *miR-497*, *miR-195*) in the MM region that target genes with phenoconnectivity to muscle physiology. Finally, the genetic variation underlying MM could be acting via *trans*-regulatory effects on other genes with physiological roles in muscle development, including excellent candidates that are just ~500 kb proximal to the MM interval (e.g., myosin, heavy polypeptide 3, skeletal muscle, embryonic; *myh3*). Disruption of *myh3* results in reduced muscle mass similar to what is observed in MM (Acakpo-Satchivi et al. 1997; Allen et al. 2001) and a missense mutation in this gene results in autosomal dominant myopathy in humans (Martinsson et al. 2000). A polymorphism within the MM region could have regulatory effects on this closely adjacent gene or on unlinked genes that regulate muscle.

In summary, a recessive MM mutation causing reduced hindlimb muscle mass in mice has been mapped to a 2.6335-Mb interval on MMU11 containing ~100 genes, many of which have known roles in muscle development. Identification of the genetic variation that underlies MM could potentially be very important in understanding both normal muscle function and dysregulation of muscle physiology leading to disease. However, finding the DNA polymorphisms that cause MM will be very challenging given the gene density and complexity of the mapped region.

Funding

United States National Science Foundation (IOB-0543429 to T.G.); the National Institutes of Health (DK076050 to D.P.).

Acknowledgments

We are grateful to Kunjie Hua and Ryan Gordon for laboratory assistance and to Peter Sorensen for help with data management. We appreciate useful feedback from Bruce Aronow regarding the miRNAs discussed in the paper.

References

- Acakpo-Satchivi LJ, Edelmann W, Sartorius C, Lu BD, Wahr PA, Watkins SC, Metzger JM, Leinwand L, Kucherlapati R. 1997. Growth and muscle defects in mice lacking adult myosin heavy chain genes. *J Cell Biol.* 139:1219–1229.
- Allen DL, Harrison BC, Sartorius C, Byrnes WC, Leinwand LA. 2001. Mutation of the IIB myosin heavy chain gene results in muscle fiber loss and compensatory hypertrophy. *Am J Physiol Cell Physiol.* 280:C637–C645.
- Allan MF, Eisen EJ, Pomp D. 2005. Genomic mapping of direct and correlated responses to long-term selection for rapid growth rate in mice. *Genetics.* 170:1863–1877.
- Bradford GE, Famula TR. 1984. Evidence for a major gene for rapid postweaning growth in mice. *Genet Res.* 44:293–308.
- Garland T Jr. 2003. Selection experiments: an under-utilized tool in biomechanics and organismal biology. In: Bels VL, Gasc JP, Casinos A, editors. *Vertebrate biomechanics and evolution.* Oxford: BIOS Scientific Publishers. p. 23–56.
- Garland T Jr, Morgan MT, Swallow JG, Rhodes JS, Girard I, Belter JG, Carter PA. 2002. Evolution of a small-muscle polymorphism in lines of house mice selected for high activity levels. *Evolution.* 56:1267–1275.
- Godfrey P, Rahal JO, Beamer WG, Copeland NG, Jenkins NA, Mayo KE. 1993. GHRH receptor of little mice contains a missense mutation in the extracellular domain that disrupts receptor function. *Nat Genet.* 4:227–232.
- Guderley H, Houle-Leroy P, Diffie GM, Camp DM, Garland T Jr. 2006. Morphometry, ultrastructure, myosin isoforms, and metabolic capacities of the “mini muscles” favored by selection for high activity in house mice. *Comp Biochem Physiol Part B.* 144:271–278.
- Guderley H, Joannis DR, Mokas S, Bilodeau GM, Garland T Jr. 2008. Altered fiber types in gastrocnemius muscle of high wheel-running selected mice with mini muscle phenotypes. *Comp Biochem Physiol B.* 149:490–500.
- Hannon RM, Kelly SA, Middleton KM, Kolb EM, Pomp D, Garland T Jr. 2008. Phenotypic effects of the “mini-muscle” allele in a large HR x C57BL/6J mouse backcross. *J Heredity.* doi: 10.1093/jhered/esn011.
- Horvat S, Medrano JF. 2001. Lack of *Socs2* expression causes the high-growth phenotype in mice. *Genomics.* 72:209–212.
- Houle-Leroy P, Guderley H, Swallow JG, Garland T Jr. 2003. Artificial selection for high activity favors mighty mini-muscles in house mice. *Am J Physiol Regul Integr Comp Physiol.* 284:R433–R443.
- Kelly SA, Czech PP, Wight JT, Blank KM, Garland T Jr. 2006. Experimental evolution and phenotypic plasticity of hindlimb bones in high-activity house mice. *J Morphol.* 267:360–374.
- Lee HJ, Göring W, Ochs M, Mühlfeld C, Steding G, Paprotta I, Engel W, Adham IM. 2004. *Sox15* is required for skeletal muscle regeneration. *Mol Cell Biol.* 24:8428–8436.
- Martinsson T, Oldfors A, Darin N, Berg K, Tajsharghi H, Kyllerman M, Wahlstrom J. 2000. Autosomal dominant myopathy: missense mutation (Glu-706 → Lys) in the myosin heavy chain IIa gene. *Proc Natl Acad Sci USA.* 97:14614–14619.
- Mason AJ, Hayflick JS, Zoeller RT, Young WS 3rd, Phillips HS, Nikolics K, Seeburg PH. 1986. A deletion truncating the gonadotropin-releasing hormone gene is responsible for hypogonadism in the hpg mouse. *Science.* 234:1366–1371.
- McPherron AC, Lawler AM, Lee SJ. 1997. Regulation of skeletal muscle mass in mice by a new TGF-beta superfamily member. *Nature.* 387:83–90.
- Quiram PA, Ohno K, Milone M, Patterson MC, Pruitt NJ, Brengman JM, Sine SM, Engel AG. 1999. Mutation causing congenital myasthenia reveals acetylcholine receptor beta/delta subunit interaction essential for assembly. *J Clin Invest.* 104:1403–1410.

- Rezende EL, Gomes FR, Malisch JL, Chappell MA, Garland T Jr. 2006. Maximal oxygen consumption in relation to subordinate traits in lines of house mice selectively bred for high voluntary wheel running. *J Appl Physiol.* 101:477–485.
- Swallow JG, Carter PA, Garland T Jr. 1998. Artificial selection for increased wheel-running behavior in house mice. *Behav Genet.* 28:227–237.
- Swallow JG, Rhodes JS, Garland T Jr. 2005. Phenotypic and evolutionary plasticity of organ masses in response to voluntary exercise in house mice. *Integr Comp Biol.* 45:426–437.
- Syme DA, Evashuk K, Grintuch B, Rezende EL, Garland T Jr. 2005. Contractile abilities of normal and “mini” triceps surae muscles from mice (*Mus domesticus*) selectively bred for high voluntary wheel running. *J Appl Physiol.* 99:1308–1316.
- Szabó G, Dallmann G, Müller G, Patthy L, Soller M, Varga L. 1998. A deletion in the myostatin gene causes the compact (Cmpt) hypermuscular mutation in mice. *Mamm Genome.* 9:671–672.
- Varga L, Szabó G, Darvasi A, Müller G, Sass M, Soller M. 1997. Inheritance and mapping of Compact (Cmpt), a new mutation causing hypermuscularity in mice. *Genetics.* 147:755–764.
- Zhang Y, Proenca R, Maffei M, Barone M, Leopold L, Friedman JM. 1994. Positional cloning of the mouse obese gene and its human homologue. *Nature.* 372:425–432.

Received March 7, 2008

Accepted April 17, 2008

Corresponding Editor: Susan J. Lamont